MODELLING OF DYNAMIC STABILITY DERIVATIVES USING CFD

Sean Tuling
CSIR

Keywords: *Navier-Stokes, CFD, Dynamic Derivatives*

Abstract

An exploratory investigation into the use of a commercial Navier-Stokes time accurate code, Fluent, for simulating and predicting the combined pitch damping derivatives, $C_{m_q}+C_{m_{\dot{\alpha}}}$, was conducted.

The stable store, a low l/d finned missile like configuration, was used for the investigation. The derivatives were extracted from the response of the store, which was simulated by providing a initial disturbance and allowing the store to oscillate freely at the system natural frequency. The same setup, as used for the numerical simulations, was used for the experimental simulations.

Static steady state runs were initially performed, and compared favourably to experimental results providing confidence in the mesh and solver parameters.

The results of the numerical simulations did not compare favourably with the experimental results. The numerical investigations (both inviscid and viscous) overpredicted the derivatives compared to the experimental results by a factor of three. The time taken for the simulations was considered reasonable.

The two main factors that need to be investigated, which may be causing the poor correlation, are the time step size and the experimental apparatus sting effects.

List of Symbols

c	Damping force, $Nm.(deg/s)^{-1}$
C_A	Store axial force coefficient
C_m	Moment coefficient about the store y body axis
C_{m_q}	Moment coefficient about the store body pitch axis due to pitch velocity, $\frac{\partial C_m}{\partial \frac{ql}{2V}}$, rad^{-1}
$C_{m_{\dot{\alpha}}}$	Moment coefficient about the store body pitch axis due to time rate change of angle of attack, $\frac{\partial C_m}{\partial \frac{\dot{\alpha}l}{2V}}$, rad^{-1}
C_N	Store normal force coefficient
F	Force
I	Mass moment of inertia, $kg.m^2$
$K_{support}$	Support or flexure stiffness/spirng constant, $Nm.deg^{-1}$
l	Reference length, m
M	Mach number
q	Angular time rate of change about the store y body axis, $rad.s^{-1}$
rf	Reduced frequency, $\frac{\omega l}{2V}$
S	Reference Area, m^2
V	Free-stream velocity, $m.s^{-1}$
α	Angle of attack, degrees
ρ	Freestream air density, $kg.m^{-3}$
θ	Angle about the store body pitch axis

Nomenclature

CFD	Computational Fluid Dynamics
LSWT	Low Speed Wind Tunnel
MSWT	Medium Speed Wind Tunnel

1 Introduction

In the process of designing and engineering a flight vehicle to meet stated specifications and objectives, the prediction of aerodynamics loads is required for structural stressing, and the prediction of performance and stability and handling. Of the many sub-disciplines in aeronautical engineering, flight load load prediction is one of the most difficult, yet one of the primary inputs to achieving efficient and safe flight.

Non-experimental prediction methodologies have matured over the last 100 years of power manned flight, to the extent where time independent or steady state predictions compare favourably with experimental predictions. The time dependent or dynamics stability derivative predictions are, however, inadequate. Probably the best available prediction techniques available are semi-empirical. Characterisation of dynamics stability derivatives are, however, still obtained experimentally, even though the experimental techniques provide limited information. Recently, attempts using lower order computational techniques have yielded limited success [1], pointing towards the complex flow mechanisms involved in time dependent responses for flight vehicles. It would thus be appropriate to attempt to use higher order techniques to develop prediction capabilities.

The modelling and simulation of dynamic stability derivatives using the Navier-Stokes computational fluid dynamics (CFD) approach is a current research topic. This is a natural extension of the maturation of Navier-Stokes CFD as a prediction technique, firstly in in modelling steady state or time averaged/independent cases and then unsteady or time dependent cases.

To this end, an exploratory investigation of using CFD to model dynamic stability derivatives was initiated, with a view to developing a prediction capability. The exploratory investigation is the topic of this paper. The results of the investigation are compared to experimental data.

A number of previous attempts at predicting dynamic stability derivatives have been attempted. Weinacht [2],[3],[4] used the lunar coning methodology to predict the pitch damping derivatives for a ballistic shell in the supersonic flight regime. This method reduces the unsteady, moving geometry problem to a static steady state case, though the frame of reference needs to be transformed.

Murman [5] has used the reduced frequency technique to predict the dynamic stability derivatives for the standard dynamics model for the sub- and transonic Mach numbers, the basic finner missile in the supersonic regime, and modified finner missile configuration for transonic and supersonic flight regimes. The reduced frequency method represents the response of a vehicle with a small predictable number of frequency components.

Green *et al* [1] attempted to use a time dependent panel method code to predict the dynamic stability derivatives for the F16XL configuration. The code, however, failed to capture the basic and essential features of the experimentally measured dynamic data for the F16XL configuration.

One of the unique features of the exploratory investigation was to perform the simulations using commercially available codes such as CFD-RC Fastran and Fluent. The simulations are thus time dependent (in contrast to the above mentioned methods).

The code chosen was Fluent. Fluent has a time accurate moving body capability, requires an unstructured tetrahedral mesh, while the motion is simulated using a user-defined function.

This paper details the attempt in simulating the pitch dynamic stability derivatives $C_{m_q} + C_{m_{\dot{\alpha}}}$ with a Navier-Stokes CFD code, Fluent, using the time dependent free oscillation technique, of the stable store configuration at low subsonic conditions, and comparing these to experimentally obtained results. The question of whether the dynamic stability derivatives can reasonably (without significant computational effort) be simulated using the time dependent free oscillation technique using Fluent was being investigated. Successful prediction can provide a useful prediction tool for the conceptual or initial design phase.

2 Dynamic Stability Derivatives

The aerodynamic loads on a flight vehicle are traditionally expressed as a first order Taylor series of derivatives [6]. For example, in coefficient form, the pitching moment, C_m can be expressed as:

$$C_m = \frac{\partial C_m}{\partial \alpha}\alpha + \frac{\partial C_m}{\partial \beta}\beta + \ldots + \frac{\partial C_m}{\partial q}q + \frac{\partial F}{\partial \dot{\alpha}}\dot{\alpha} + \ldots \quad (1)$$

The derivatives of interest are the time rate dependent derivatives, namely C_{m_q} and $C_{m_{\dot{\alpha}}}$ and so forth.

The two longitudinal dynamic stability derivatives that are of greatest interest are C_{m_q} and $C_{m_{\dot{\alpha}}}$. Experimental apparatus require complex mechanisms to measure C_{m_q} alone. The most common technique employed is to measure the combined derivative $C_{m_q} + C_{m_{\dot{\alpha}}}$ by simply oscillating the model about the centre of gravity i.e. a single rotational degree of freedom. The derivative $C_{m_{\dot{\alpha}}}$ can be obtained from a second test (utilising different apparatus) by heaving the model up and down. The derivative C_{m_q} is then simply the difference between the combined derivative and $C_{m_{\dot{\alpha}}}$. For the purposes of the exploratory investigation only the combined derivative was simulated.

2.1 Experimental Prediction of Dynamic Stability Derivatives

Since the most accurate simulation method of obtaining dynamic stability derivatives has been experimental, a large number of techniques have been developed. This has further been exacerbated by the limited capabilities of experimental techniques, simply due to mechanical and measurement constraints. The most common techniques used the free and forced oscillation methods [7].

The free oscillation technique essentially provides an initial disturbance to the model in the plane or about the axis of interest and allows the model to respond without interference. The response of the model is easily modelled as a second system from which the derivatives of interest are extracted. Varying the frequency to characterize the derivative as a function of reduced frequency is, however, more difficult, requiring changes in the system stiffness or model inertia. For most free oscillation tests, the support system has a stiffness (in the form of a flexure) which can be used to control the natural frequency, in combination with the model inertia, to the desired value.

The forced oscillation technique forces the model to oscillate at the required frequency, from which derivatives can be extracted from the time response of the system and model. The experimental apparatus is, however, an order of magnitude more complex than for a free oscillation test, since the apparatus needs to control the model oscillation amplitude and frequency, whereas the free oscillation technique only requires a trigger mechanism.

2.2 Governing Equations

The equation of motion describing the single degree of freedom is expressed as:

$$I\ddot{\theta} + c\dot{\theta} + k\theta = F \quad (2)$$

For the method used is this investigation, $F = 0$ i.e. free oscillation, and $c \equiv C_{m_q} + C_{m_{\dot{\alpha}}}$. I is the moment of inertia of the store and K is the spring constant of the system.

The spring constant of the system is algebraic sum of the support stiffness and pitching moment due to angle of attack variation, C_{m_α} i.e. $K \equiv K_{support} + C_{m_\alpha}$.

The system response, or solution to the equation of motion 2 can be written as:

$$\theta = \theta_0 e^{\frac{c}{2I}t}\cos(\omega_d t + \phi) \quad (3)$$

where θ_0 and ϕ are arbitrary constants, and ω_d is the damped natural frequency.

The combined damping derivative $C_{m_q} + C_{m_{\dot{\alpha}}}$ is thus obtained by non-dimensionalised the damping force c by $\frac{\frac{1}{2}\rho V^2 S l^2}{2V}$, where $\frac{1}{2}\rho V^2$ is the freestream dynamic pressure and S is the reference area.

Dynamic stability derivatives have also been shown to be dependent on frequency, this represented by the non-dimensional reduced frequency parameter, rf. The reduced frequency is defined as:

$$\mathrm{rf} = \frac{\omega l}{2V} \tag{4}$$

where ω is the frequency of oscillation, l is the reference length and V is the freestream velocity.

Thus simulations would be required to show the dependence of the derivatives with reduced frequency.

The amplitude of the oscillations conformed to the small amplitude criteria i.e. less than 3 degrees.

3 Research Programme

To minimise the variations between the numerical and experimental simulations, the numerical simulations were performed under similar freestream conditions as for the experimental simulations. Furthermore, the same model inertias, support system stiffness and similar oscillating amplitudes were used, thus also removing any scaling inaccuracies.

The experimental method chosen for this investigation is the free oscillation technique with a support system stiffness in the form of a flexure that is used to also measure the model response.

The configuration chosen to perform the numerical and experimental simulations was the stable store. This is a simple body finned missile type configuration, has a low length to diameter ratio and is illustrated in Figure 3. The centre of gravity is mid centre of the length of the store (or 215.9mm from the store nose). The fins configuration used was in the cross and not the plus configuration. All dynamic derivative simulations were performed around the store steady state angle of attack of 0°. The initial pertubation angle was 0.3°. The store was oscillated about the centre of gravity, this being the mid centre of the length of the store.

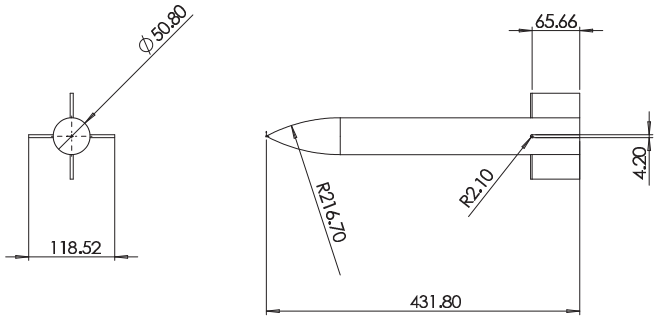

Fig. 1 Stable Store configuration

4 CFD Modelling

4.1 Modelling Process

A two step modelling process was followed whereby the mesh was first validated for the steady state case and then the same mesh was used for the transient or moving mesh simulations. The effects of viscosity were also investigated by comparing results for the dynamic stability derivative simulations between the inviscid case and a viscous case using a turbulence model. The turbulence model used was the standard κ-ω as implemented in Fluent.

No mesh size dependency was considered for the unsteady runs. The mesh that was used was, however, determined to be mesh independent in steady state by running cases with more refined meshes without any appreciable changes in the results. Additionally, no grid adaption was applied to the mesh for the steady state cases.

4.2 Mesh Generation

The mesh, being unstructured and using tetrahedral cells, was automatically generated in Gambit using the following parameters

- Fin edge curvature maximum angle of 20°
- Body and in face cell size of 4mm
- Growth rate of 1.2

This resulted in a mesh of approximately 610000 cells for the inviscid simulations. The mesh domain is illustrated in figure 4.2, while figure 4.2 shows the mesh around the store.

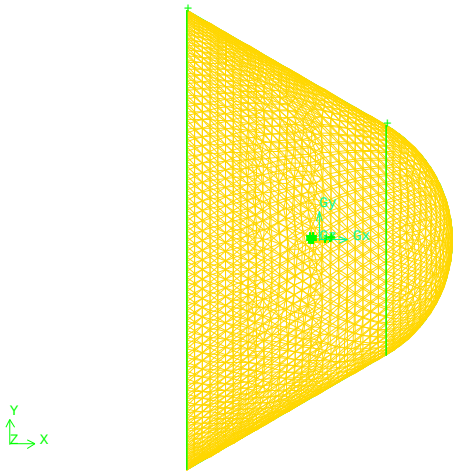

Fig. 2 Fluid Domain

A boundary layer was attached for the viscous runs using the following parameters

- Cell size of 0.4mm
- Growth rate 1.1

The resulting mesh was approximately 1130000 cells.

The turbulence parameters used for the simulations are listed in the table 1.

The far field boundary conditions used were pressure-far-field for the inlet and pressure-outlet for the outlet.

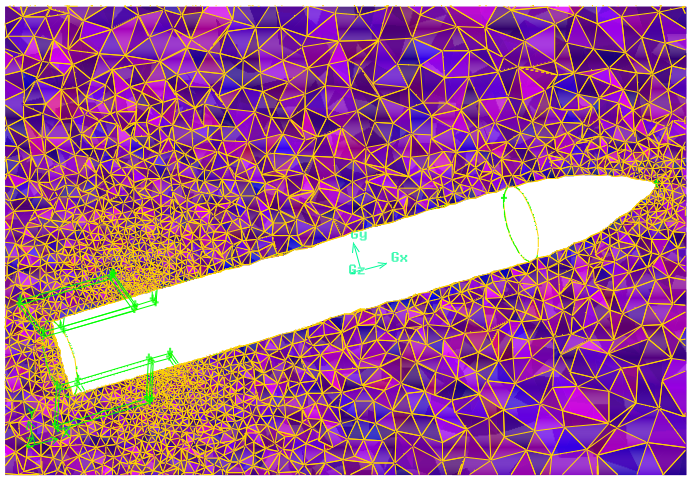

Fig. 3 Mesh around the store

Table 1 Turbulence Parameters

Parameter	Value
Turbulence Intensity	0.1%
Turbulence Length Scale	0.0005m

4.3 Steady State Validation

The mesh was validated in steady state against experimental data for both the inviscid and viscous cases. The coefficients of interest are the normal force, C_N, and the pitching moment, C_m. Correlation of the axial force, C_A, was not considered.

The experimental data were obtained, in the Medium Speed Wind Tunnel (MSWT) of the CSIR, under the following conditions:

- Mach number, M=0.4
- Total pressure, $P_T = 150kPa$
- Total temperature, $T_T = 310K$

Because the flow physics over the model is dominated by potential flow, little differences were expected between the inviscid solution and those using the turbulence model.

Figures 4.3 and 4.3 show the comparison of the viscous and inviscid solutions against the ex-

perimental data. As expected, the viscous and inviscid solutions are similar.

For the viscous runs the y^+ values varied between 50 and 250.

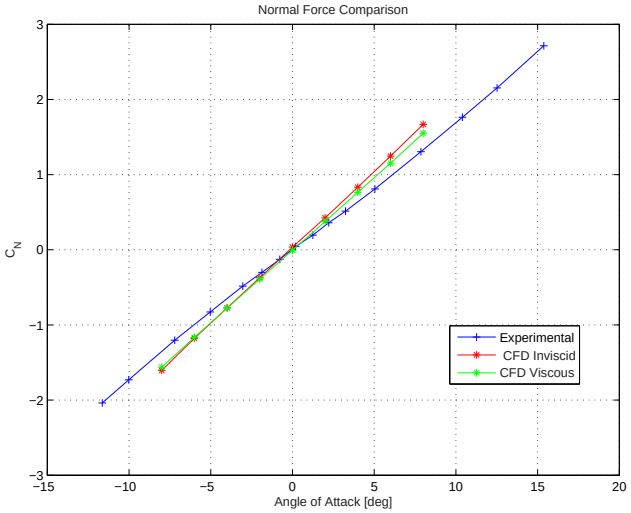

Fig. 4 Steady state case comparison of normal force coefficient, C_N, for inviscid, viscous and experimental data

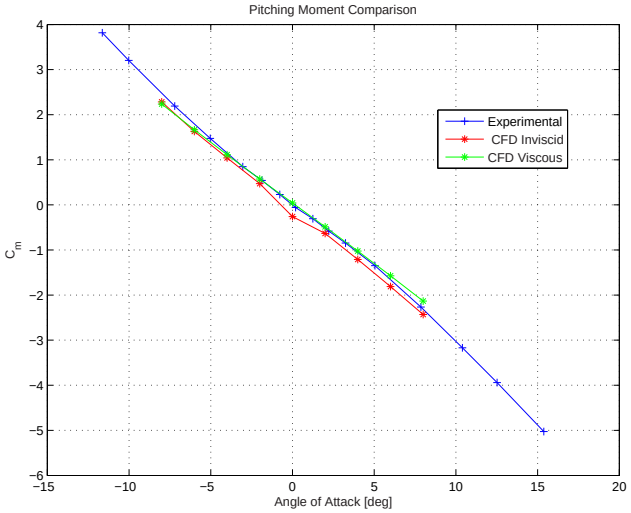

Fig. 5 Steady state case comparison of pitching moment coefficient, C_m, for inviscid, viscous and experimental data

4.4 Dynamic Stability Derivative Simulations

The dynamic derivative simulations were performed as for the experimental simulations.

The moving mesh parameters used for the simulation were as follows:

- Segregated solver
- Time step of 5×10^{-5} seconds (or 0.00005s)
- PISO pressure-velocity coupling

The simulations were performed for at least one and a half cycles, from which $C_{m_q} + C_{m_{\dot{\alpha}}}$ were extracted by curve fitting the response to the solution of the equations of motion (as described in 3).

4.5 Time Step Sizing

The determination of time step size was dictated by the compromise between capturing time dependent phenomena, time step independent results and run time. The time step size determined for the simulations was 0.00005 seconds.

This time step size is such that time dependent phenomena varying at the same frequency as the natural frequency would propagate through no more than four average sized tetrahedral cells between each time step. The average cell size was for cells at the surface of the store for the inviscid simulations and for cells adjacent the boundary layer for the viscous simulations. Flow phenomena at the fin leading edges would thus propagate through more than four cells between each time step because of the cell refinement.

The dependence of the results on time step was also assessed by performing simulations for varying time steps at M=0.1 for the inviscid case. This was not performed for the viscous case. The derivative for three time steps are shown in table 2.

From the table above, no significant change in results were expected for a time step below 0.00005 seconds.

Table 2 Time Step Size Comparison

Time [sec]	$C_{m_q}+C_{m_{\dot{\alpha}}}$
0.001	-321.9
0.0001	-290.6
0.00005	-282.6

4.6 Experimental Programme

The experimental simulations were performed in the Low Speed Wind Tunnel (LSWT) of the CSIR. The freestream conditions for the dynamic derivative simulations are low subsonic, where the Mach number varies from about M=0.05 to M=0.13. The static pressure was at atmospheric or about 87kPa, while the static temperature was approximately 300K. Actual tunnel conditions were, however, used for the data processing and reduction.

At least 10 simulations were obtained for each tunnel and store configuration to ascertain the uncertainty in the measured derivative. The maximum uncertainty was estimated at $\Delta(C_{m_q}+C_{m_{\dot{\alpha}}})=10$.

4.7 Observations and Results

A typical time response for the oscillations is shown in figure 4.7.

The results for the dynamic derivative simulations are shown in figure 4.7. The figure shows the comparison of the inviscid, viscous and experimental pitch dynamic stability derivatives, $C_{m_q}+C_{m_{\dot{\alpha}}}$, as a function of the reduced frequency.

The numerical simulations show no discernable dependence on the reduced frequency, rf. Additionally the effect of viscosity also seems to be negligible from the results. Of particular concern, however, is that the numerical simulations overpredict the damping, by approximately 3 times.

The calendar time taken to perform a numerical simulation for 2 cycles was approximately 3 days for the inviscid runs, and 6 days for the viscous runs. The runs were performed on a cluster, where each simulation was executed across 4 nodes.

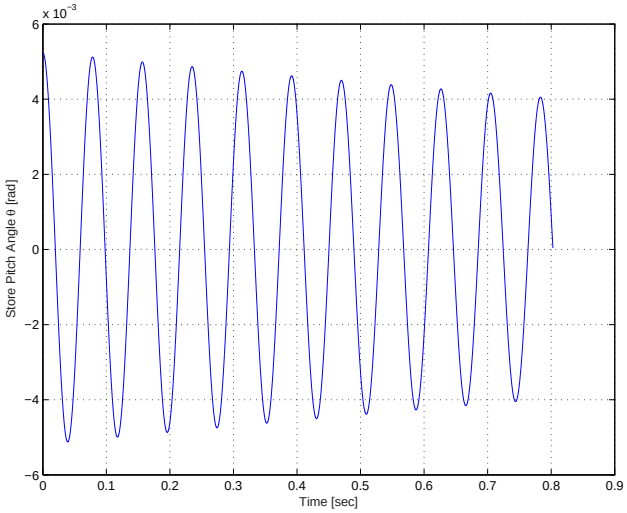

Fig. 6 Typical store response

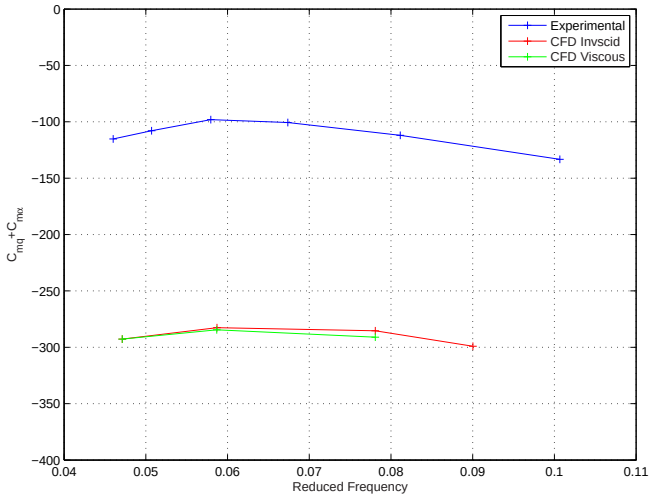

Fig. 7 Comparison of the numerical and experimental pitch damping derivative,$C_{m_q}+C_{m_{\dot{\alpha}}}$

5 Discussion

5.1 Steady State

The static steady state numerical solutions correlated well with the experimental data. This provided confidence in the mesh being able to capture the dominant flow characteristics of the configuration. The inviscid solution, as expected,

overpredicted the normal force more than the viscous solution.

5.2 Dynamic Simulations

From figure 4.7 it is quite clear that the numerical simulations are overpredicting the damping. No obvious cause for this has been identified. The same overprediction is, however, observed by Murman [5] in their comparison of the basic finner configuration with wind tunnel data (overprediction by a factor of 2), where they attributed their overprediction to sting effects. No sting effects were measured or considered for the experimental simulations, and thus the experimental simulations could be underpredicting the dynamic stability derivatives.

The dependence of the dynamic derivatives on the reduced frequency was not negligible or insignificant in the experimental simulations. The numerical results seem to show the same trend, though the dependency is of secondary concern especially considering the magnitude of the overprediction.

5.2.1 Time Step Size and Simulation Time

The time step size was calculated such that flow phenomena of the same frequency as the system natural frequency would not propagate through the mesh faster than three or four average cells at a time for each time step.

The time taken per simulation is two orders of magnitude higher than for static steady state simulations. The cost is, thus not negligible or trivial and was considered when performing the simulations.

The time step size could be higher than that required to capture the time dependent effects, and is definitely not capturing any effects whose frequencies are higher than that of the system natural frequency. Additionally phenomena around the fin leading edges would be less well captured that in other areas because of the cell refinement in that area.

A reduction of the time step to at least 1×10^{-6} seconds is thus recommended and the simulations rerun to ascertain the effects of the time step reduction. This will, however, increase the time for the simulations by two orders of magnitude.

5.2.2 Mesh Dependency

No mesh dependency studies were performed for the dynamic simulations. Even though the static steady simulations were acceptable for the mesh implemented, its effect on the dynamic simulation remains unknown. It is recommended that this aspect also be investigated.

6 Conclusions and Recommendations

An exploratory investigation into the use of a commercial Navier-Stokes time accurate code, Fluent, for simulating and predicting the combined pitch damping derivatives, $C_{m_q} + C_{m_{\dot{\alpha}}}$, was conducted. The study simulated the response of the stable store using the free oscillation technique both numerically and experimentally. Additionally for the numerical and experimental simulations, the store size was identical and the freestream flight conditions similar. The results showed an overprediction of the numerical derivatives by a factor of three compared to the experimental results.

It can be concluded that the numerical simulations do not compare favourably with the experimental simulations. The use of Fluent and the free-oscillation test technique does not yield sufficiently good results, for the stable store configuration with the applied simulation parameters, to be used for even the initial design process. Increased simulation time (beyond that which is reasonable) may be required to capture the time dependent effects for the simulations to be usable.

A number of aspects need to be investigated to improve the accuracy of the numerical simulations and correlation between the numerical and experimental . These are recommended below.

6.1 Recommendations

The following are recommended:

- Investigate the effect of sting interference on the experimental investigations
- Reduce the time step to at least 1×10^{-6} seconds and rerun the simulations
- Determine the effect of mesh size on the dynamic stability derivative predictions

References

[1] Green L.L, Spence A.M. and Murphy P.C. Computational Methods for Dynamic Stability and Control Derivatives. *42nd AIAA Aerospace Sciences Meeting*, 2004. AIAA 2004-0015.

[2] Weinacht P, Sturek W.B. and Schiff L.B. Navier-Stokes Predictions of Pitch Damping for Axisymmetric Projectiles. *Journal of Spacecraft and Rockets*, Vol. 34, No. 6, 1997.

[3] Weinacht P. Navier-Stokes Predictions of the Individual Components of the Pitch-Damping Sum. *Journal of Spacecraft and Rockets*, Vol. 35, No. 5, 1998.

[4] Weinacht P. Projectile Performance, Stability, and Free-Flight Motion Prediction Using Computational Fluid Dynamics. *Journal of Spacecraft and Rockets*, Vol. 41, No. 2, 1998.

[5] Murman S.M. A Reduced-Frequency Approach for Calculating Dynamic Derivatives. *43rd AIAA Aerospace Sciences Meeting*, January 10-13, 2005. AIAA 2005-0840.

[6] Bryan G.H. *Stability in Aviation*. MacMillian, 1911.

[7] Schueler C.J, Ward L.K. and Hodapp A.E. Jr. Techniques for Measurement of Dynamic Stability Derivatives in Ground test Facilities. *Agardograph 121*, October 1967.